

Mass Spectrometry and Theoretical Investigation of VN_n^+ ($n = 8, 9,$ and 10) Clusters

Kewei Ding,^{†,‡} Hongguang Xu,[§] Yang Yang,^{||} Taoqi Li,[‡] Zhaoqiang Chen,^{||} Zhongxue Ge,^{*,†,‡} Weiliang Zhu,^{*,||} and Weijun Zheng^{*,§}

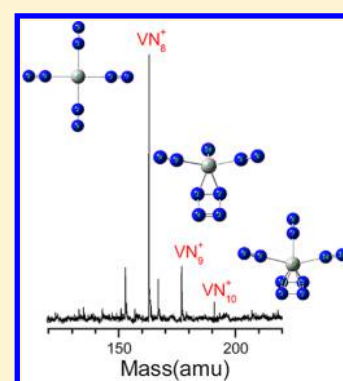
[†]State Key Laboratory of Fluorine & Nitrogen Chemicals, Xi'an 710065, China

[‡]Xi'an Modern Chemistry Research Institute, Xi'an 710065, China

[§]Beijing National Laboratory for Molecular Sciences, Institute of Chemistry, Chinese Academy of Sciences, Beijing 100190, China

^{||}Shanghai Institute of Materia Medica, Chinese Academy of Sciences, Shanghai 201203, China

ABSTRACT: VN_n^+ clusters were generated by laser ablation and analyzed by mass spectrometry. The results showed that VN_8^+ , VN_9^+ , and VN_{10}^+ clusters were formed, and the mass peak of VN_8^+ is dominant in the spectrum. The VN_8^+ cluster was further investigated by a photodissociation experiment with 266 nm photons. Density functional theory calculations were conducted at the M06-2X/6-311+G(d,p) level to search for stable structures of VN_n^+ ($n = 8, 9,$ and 10) and their neutral counterparts. The theoretical calculations revealed that the most stable structure of VN_8^+ is in the form of $V(N_2)_4^+$ with D_{4h} symmetry. The binding energy from the calculation is in good agreement with that obtained from the photodissociation experiments. The global minimum structures of VN_8 , $VN_9^{+/0}$, and $VN_{10}^{+/0}$ contain a similar substructure of the N_4 ring and exhibit energy properties. The most stable structure of VN_9^+ is in the form of $(\eta^2-N_4)V^+(N_2)_2$ with C_1 symmetry, while that of VN_{10}^+ is in the form of $(\eta^4-N_4)V^+(N_2)_3$ with C_s symmetry. For neutral VN_8 , VN_9 , and VN_{10} , $(\eta^4-N_4)V(N_2)_2$, $(\eta^4-N_4)V(N_3)(N_2)$, and $(\eta^4-N_4)V(N_2)_3$ are their ground-state structures, with decomposition into one V atom, and corresponding quantities of N_2 can release energies of about 50.20, 96.28, and 57.76 kcal/mol, respectively.



1. INTRODUCTION

The polynitrogen compounds are of significant interest as potential candidates for high-energy-density materials (HEDM).^{1,2} Their high energy content stems from the N–N single and double bonds as well as the tension rings they possess.³ Numerous theoretical^{4,5} and experimental studies have been carried out to find new polynitrogen species, but only a few efforts have been successful. Christie and co-workers synthesized the N_5^+ ion in the form of an AsF_6^- salt in 1999.⁶ Cacace and co-workers⁷ detected a N_4 isomer with open-chain structure in 2002. At about the same time, Ashwani Vij and co-workers produced N_5^- following the collision-induced dissociation of the *para*-pentazolyphenolate anion.⁸ One year later, Hansen and Wodtke⁹ reported the first evidence for the production of a ring isomer of N_3 , which is confirmed by later experimental^{10–12} and theoretical^{13,14} work. The synthesis of the N_4 ring was attempted as early as 1982 through a (2 + 2) cycloaddition reaction,^{15–20} but it was not until 2012 that Camp and co-workers detected a tetraalkyl tetrazetidinetracarboxylate radical cation,²¹ which was the first discovery of a substituted N_4 ring in experiment as far as we know.

At same time, some scientists turned their eyes to metal-doped nitrogen clusters and predicted that novel all-nitrogen units comprising cyclic N_4 ,^{22–25} N_5 ,²⁶ N_6 ,²⁷ and N_7 ²⁸ could exist in M–N clusters. This might be because the polynitrogen rings can be stabilized by the metal–ligand interaction. Cheng

and Li predicted that an alkali metal cation (Li^+ , Na^+ , K^+ , Rb^+ , or Cs^+) and N_4^{2-} ring could form bipyramidal M_2N_4 structures,²³ which are likely to be stable and to be observed experimentally due to their significant isomerization or dissociation barriers. They also calculated MN_4 pyramidal structures formed by an alkaline earth cation (Ca^{2+} , Sr^{2+} , or Ba^{2+}) and the N_4 ring.²⁴ Mercero has studied the sandwich-like complexes $(N_4MN_4)^q$ ($(M, q) = (Cr, Ni, 0), (V, Co, -1), (Ti, Fe, -2)$) with a N_4^{2-} aromatic ring.²⁵ Jin and Ding calculated a type of heterodecked sandwichlike structure $(N_3MN_5)^q$ ($(M, q) = (Ni, 0), (Co, -1), (Fe, -2)$) containing two odd-membered all-nitrogen rings (N_3 and N_5).²⁶ Tsipis and Lein calculated first-row transition-metal pentazoloto complexes.^{27,28} Choi and co-workers predicted that $Ti(N_5)_4$ is a potential nitrogen-rich, stable, high-energy-density material.²⁹ Straka and Pyykkö proposed the possible high-energy nitrogen-rich pentazolides with a very large nitrogen-to-element ratio, such as $(M(N_5)_8)^{2-}$ ($M = Cr, Mo, W$).³⁰ Duan and Li investigated MN_6 ($M = Ti, Zr, Hf, Th, Sc,$ and V) with polynitrogen rings using density functional theory calculations.³¹ Gagliardi and Pyykkö found that ScN_7 has a local minimum with C_{7v} symmetry³² and the

Received: December 10, 2017

Revised: April 25, 2018

Published: May 1, 2018

sandwich structures of N_5MN_7 ($M = \text{Ti, Zr, Hf, and Th}$) are locally stable.³³

Because of the additional advantages of M–N binary clusters in designing new structural groups, extensive work with a variety of experimental techniques has been undertaken to investigate novel metal nitrides. The binary azides, $M(N_3)_n$ of groups 4,³⁴ 5,^{35–37} 6,³⁸ 14,^{39–41} 15,^{42,43} and 16^{44,45} elements ($M = \text{Ti, Nb, Ta, Mo, and W}$) were synthesized and isolated in the experiments. $Nb^+(N_2)_n$ and $V^+(N_2)_n$ complexes were investigated by Duncan and co-workers using photodissociation spectroscopy.^{46,47} The $Rh(N_2)_4^+$ complex was studied via infrared laser photodissociation spectroscopy and theoretical calculations.⁴⁸ The structure, bonding, and vibrations of $Fe(N_2)_n$ ($n = 1–5$) were investigated by density functional theory.⁴⁹ Jin and co-workers reported the spectroscopic identification of the $[B_3(N_2)_3]^+$ complex which features the smallest π -aromatic system, B_3^+ .⁵⁰ Zhou studied the $[Gd_2N_2]$ complex and found remarkable N_2 activation and cleavage by the Gd dimer.⁵¹ In our previous work, the TiN_{12}^+ clusters were generated by laser ablation, the most stable structure of which was found to be $Ti(N_2)_6^+$ with O_h symmetry.⁵² Nevertheless, the N_3 and N_2 units studied in the above works are well known. It is still a great challenge to add new members to the polynitrogen compound family.

Vanadium, one of the early transition metals, can easily form multiple-decker sandwich structures with benzene (V_nBz_{n+1})^{53–55} and could also be encapsulated by silicon to form VSi_n clusters.^{56,57} In this study, we investigated the vanadium–nitrogen binary clusters by laser ablation and photodissociation experiments coupled with theoretical calculations in order to gain insight into the geometric structure of generated clusters and their neutral counterparts.

2. EXPERIMENTAL AND COMPUTATIONAL METHODS

2.1. Experimental Method.

The experiments were conducted on a home-built apparatus equipped with a laser vaporization supersonic cluster source and a reflectron time-of-flight mass spectrometer (TOF-MS), which has been described elsewhere.⁵⁸ Briefly, the VN_n^+ ($n = 8, 9, \text{ and } 10$) cluster cations were generated in the laser vaporization source via laser ablation of a rotating and translating disk target of a V and BN mixture (13 mm diameter, V/BN mole ratio of 2:1) with the second harmonic of a nanosecond Nd:YAG laser (Continuum Surelite II-10). The typical laser power used in this work is about 10 mJ/pulse. Nitrogen gas with ~ 4 atm backing pressure was allowed to expand through a pulsed valve (General Valve Series 9) into the source and to cool the formed clusters. The generated cluster cations were mass analyzed with the TOF-MS. To further study the structure of the VN_n^+ ($n = 8, 9, \text{ and } 10$) cluster, photodissociation experiments were employed. During the photodissociation experiments, the VN_8^+ ions were selected with a pulsed mass gate at the first space focus point of the TOF-MS, decelerated with a dc electric field, and then dissociated with 266 nm photons from another nanosecond Nd:YAG laser (Continuum Surelite II-10). The fragment ions and parent ions were then reaccelerated toward the reflectron zone and reflected to the microchannel plate (MCP) detector. The output from the MCP detector was amplified with a broadband amplifier and recorded with a 200 MHz digital card. The digital data were collected on a laboratory computer with homemade software. In photodissociation experiments on the VN_9^+ and VN_{10}^+ cluster ions,

no fragment ion was observed due to the weak mass signals of the parent ions.

2.2. Computational Method.

A quantum chemistry study was performed with Gaussian 09 at the M06-2X/6-311+G(d,p) level of density functional theory (DFT) for geometry optimization and frequency calculations.^{59–61} Every stationary point on the potential energy surface (PES) was confirmed to be local minimum-energy structure by all positive harmonic frequencies. The bond length of the N_2 molecule was calculated to verify the accuracy of our method. The calculated N–N bond length is about 1.090 Å, which is consistent with an experimental value of 1.097 Å.⁶² The binding energy is defined as

$$E_{b1} = -2[E(VN_n) - E(V) - n/2E(N_2)]/n \quad (\text{for the neutral clusters}) \quad (I)$$

$$E_{b2} = -2[E(VN_n^+) - E(V^+) - n/2E(N_2)]/n \quad (\text{for the positive clusters})$$

The formation energy is calculated with

$$\Delta_f E_1 = E(VN_n) - E(V) - n/2E(N_2) \quad (\text{for the neutral clusters}) \quad (II)$$

$$\Delta_f E_2 = E(VN_n^+) - E(V^+) - n/2E(N_2) \quad (\text{for the positive clusters})$$

Throughout this article, bond lengths are given in angstroms, bond angles are given in degrees, and relative energies are given in kcal/mol.

3. RESULTS

3.1. Experimental Results.

Figure 1 shows a typical mass spectrum of clusters generated in our experiment. It can be

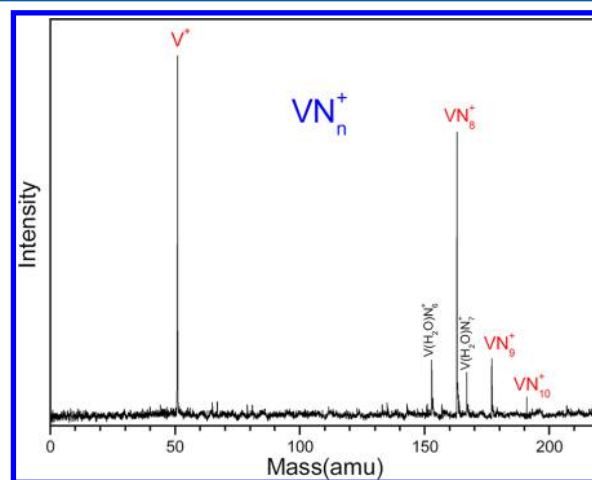


Figure 1. Typical mass spectrum of V–N clusters generated by laser ablation of a V/BN mixture target.

seen that the main mass peaks are V^+ , VN_8^+ , VN_9^+ , VN_{10}^+ , $V(H_2O)_6^+$, and $V(H_2O)_7^+$. The signal intensity of VN_8^+ is predominant compared to that of other vanadium–nitrogen clusters, which indicates that VN_8^+ may have the most stable or most symmetric structure in comparison to other clusters.

The photodissociation of VN_8^+ was conducted with 266 nm photons. The products were VN_2^+ and V^+ fragment ions as shown by the mass spectrum in Figure 2, among which the

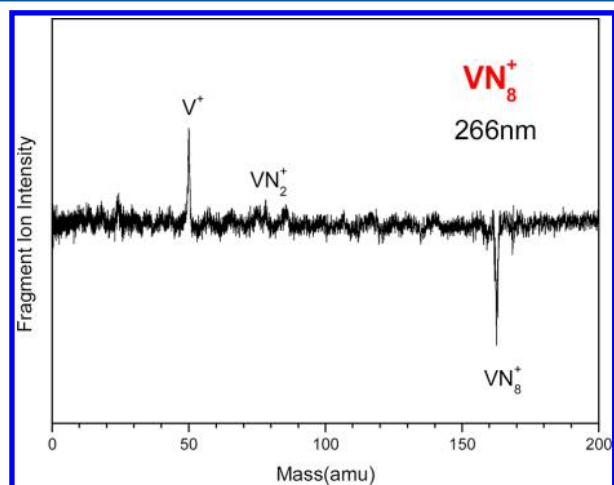


Figure 2. Photodissociation mass spectrum of the VN_8^+ cluster at 266 nm.

abundance of V^+ is much higher. The result shows that the main dissociation channel is the loss of eight nitrogen atoms and the secondary channel is the loss of six nitrogen atoms. We also tried to conduct the photodissociation of VN_9^+ and VN_{10}^+ , but no fragment ions were observed because of their weak mass signal.

3.2. Theoretical Results. To search for the stable states of VN_n^+ and VN_n ($n = 8, 9,$ and 10), we have conducted calculations for nine different systems, from VN_2 to VN_{10} . From the simplest system with two nitrogen atoms and vanadium, we designed the initial structures and found the geometrical structures of the lowest total energy states of each of them (data not shown). Then, by adding one nitrogen each time to the system, we got more and more geometrical configurations as the system became larger. By putting the nitrogen in different locations, we designed initial geometrical configurations of N_2 molecules, the N_3 chain and ring, and the $\text{N}_4, \text{N}_5, \text{N}_6,$ and N_7 rings and so on with vanadium atoms. To ensure that we obtained a true minimum at the PES as a result of the geometry optimization, we performed frequency calculations on the optimized geometries for all of them. This strategy of defining the initial geometries can avoid overlooking any possible initial structures. For each initial geometrical configuration, we also considered many spin multiplicities (2, 4, and 6 for neutral clusters and 1, 3, and 5 for positive clusters).

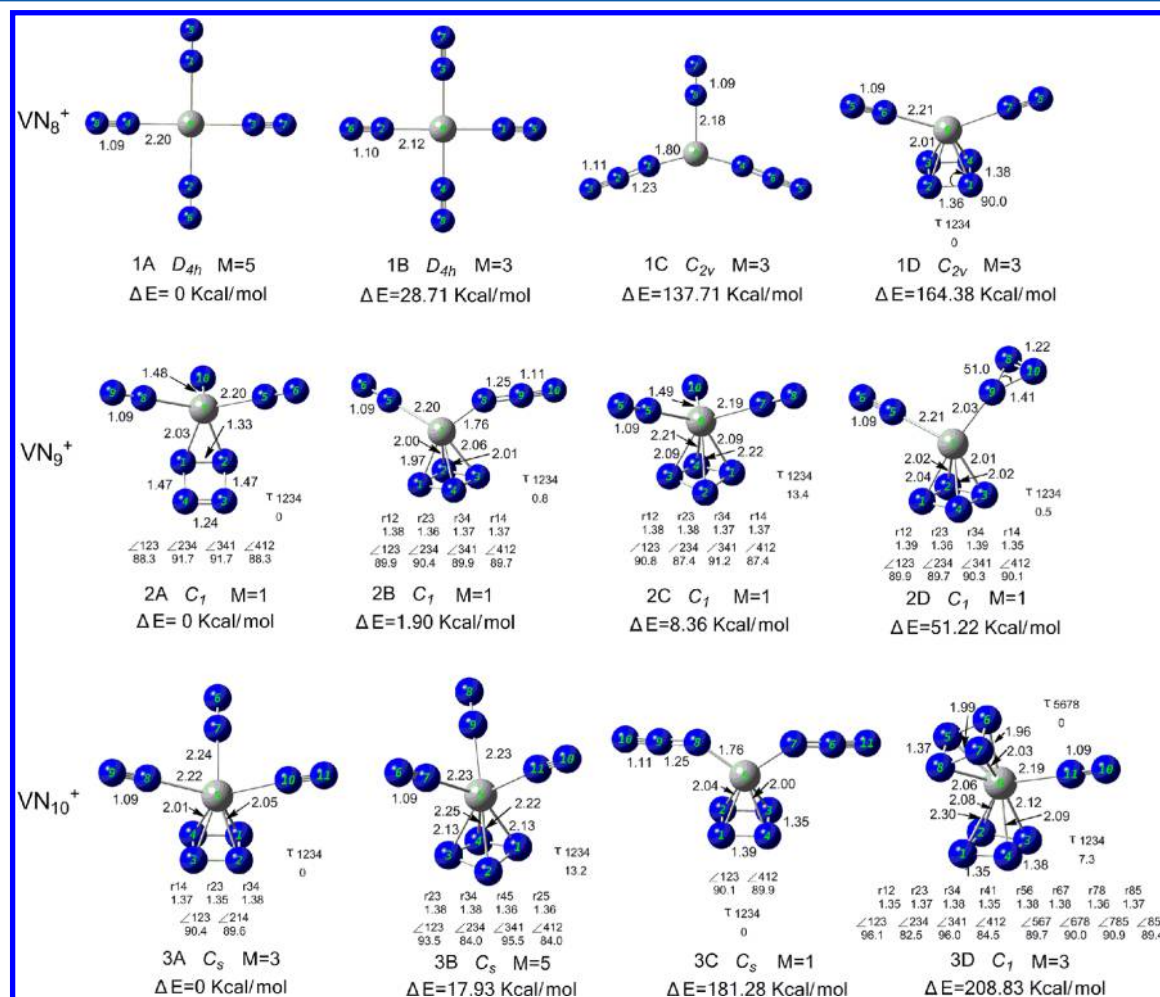


Figure 3. Structures and relative energies of the low-lying isomers of VN_n^+ ($n = 8, 9,$ and 10) clusters. Bond lengths, angles, torsion angles of the planar ring (τ), symmetry, spin multiplicity (M), and ΔE are shown.

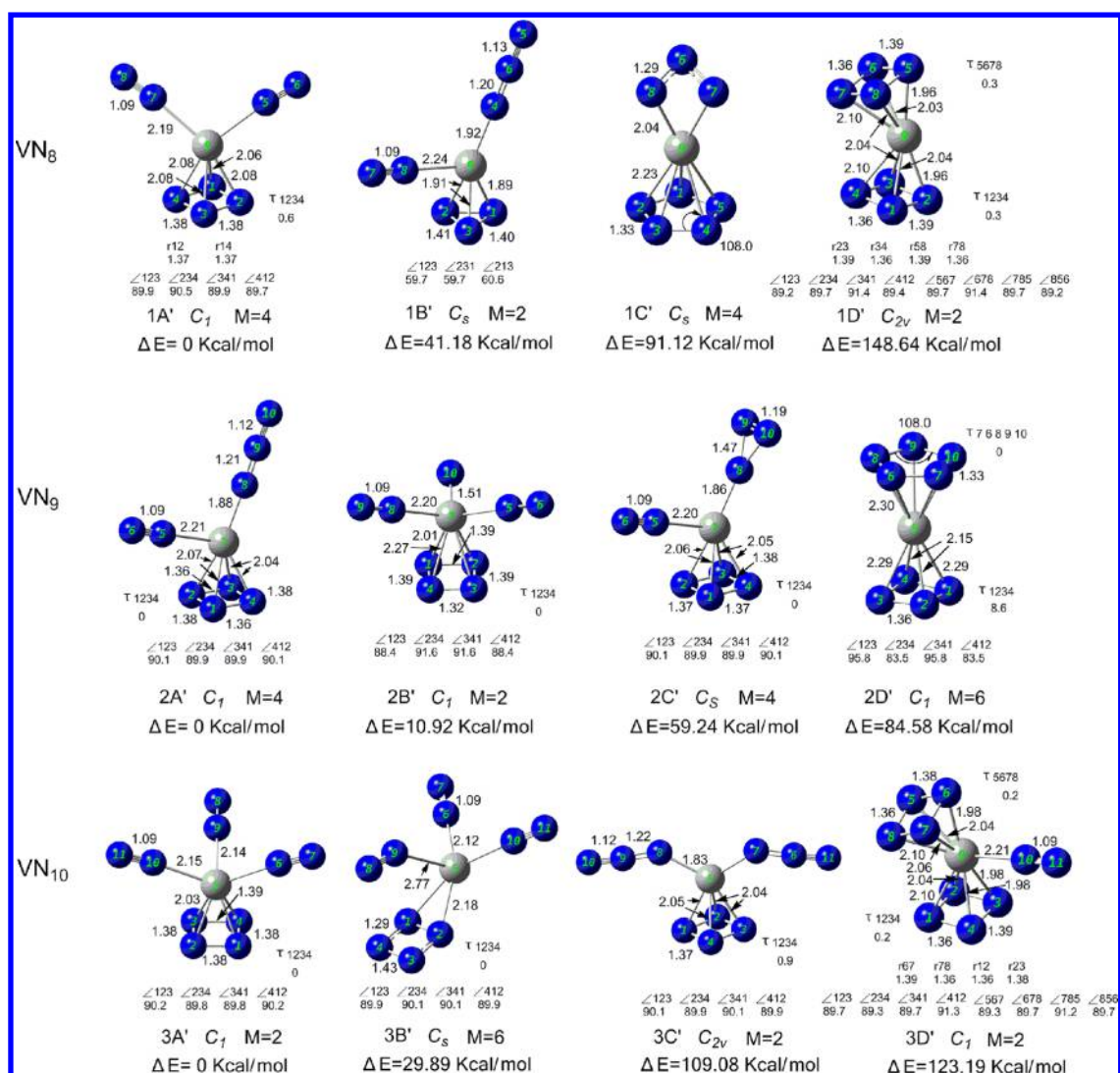


Figure 4. Structures and relative energies of the low-lying isomers of VN_n ($n = 8, 9,$ and 10) clusters. Bond lengths, angles, torsion angles of the planar ring (τ), symmetry, spin multiplicity (M), and ΔE are shown.

After full relaxation, a rather large number of low-lying isomers of VN_n^+ and VN_n ($n = 8, 9,$ and 10) were found. Here, we show the typical isomers of VN_n^+ ($n = 8, 9,$ and 10) in Figure 3 with the most stable structures on the left and those of VN_n ($n = 8, 9,$ and 10) in Figure 4. The calculated relative energies, binding energies, and formation energies of these low-lying isomers are summarized in Table 1.

3.2.1. Structures of VN_8^+ and VN_8 . The calculated ground state of VN_8^+ (1A) has planar structure with D_{4h} symmetry in which four N_2 molecules interact equally with the central vanadium atom via their terminal nitrogen atoms. The N–N bond lengths in the N_2 units are 1.09 Å, equal to that of nitrogen molecules calculated in this work. Each V– N_2 distance is 2.20 Å. The second most stable isomer (1B) has a structure similar to that of 1A except that the V– N_2 distance is shortened to 2.12 Å. Accordingly, the energy of isomer 1B increases 28.71 kcal/mol compared to that of isomer 1A. The differences in the structures of 1A and 1B mainly originate from their spin multiplicity, which are 5 and 3, respectively.

Except for N_2 units, we also found other all-nitrogen ligands in low-lying isomers of VN_8^+ . For example, the third most stable structure, 1C, is formed by attaching two N_3 ligands and

one N_2 ligand to a vanadium atom. The N–N bond length in the N_2 molecule is also 1.09 Å. The N–N bond lengths in N_3 moieties are 1.23 and 1.11 Å, which are the same as those in a typical azide. Isomer 1C is much higher in energy than isomer 1A by 137.71 kcal/mol. 1D is the most stable isomer with an all-nitrogen ring in VN_8^+ , which has two end-on bound N_2 molecules and one η^4-N_4 ring and exhibits C_{2v} symmetry. The N_4 ring in 1D has rectangular–planar structure with the bond lengths of N1–N2 and N2–N3 being 1.36 and 1.38 Å, respectively. The energy of isomer 1D is much higher than that of 1A by 164.38 kcal/mol.

For neutral VN_8 , the low-lying states are considerably different from their positive counterparts. The isomer with only N_2 units has not been obtained after full optimization. Isomer 1A' with two end-on bound N_2 molecules and one η^4-N_4 ring is the ground state of VN_8 . Compared to the similar structure of 1D, the N_4 ring in 1A' is distorted slightly from quadrature–planar structure and the symmetry of 1A' degenerated to C_1 . The bond lengths of N3–N2(N4) and N1–N2(N4) in the N_4 ring are 1.38 and 1.37 Å, which are shorter than the N–N single bond (1.45 Å) but much longer than the

Table 1. Relative Energies, Binding Energies, and Formation Energies of the Low-Lying Isomers of V–N Clusters

cluster		symmetry	multiplicity	ΔE (kcal/mol)	E_b (kcal/mol)	$\Delta_f E$ (kcal/mol)
VN ₈ ⁺	1A	D _{4h}	5	0	24.84	−99.36
	1B	D _{4h}	3	28.71	17.66	−70.65
	1C	C _{2v}	3	137.71	−9.59	38.34
	1D	C _{2v}	3	164.38	−16.25	65.01
VN ₈	1A'	C ₁	4	0	−12.55	50.20
	1B'	C _s	2	41.18	−22.84	91.38
	1C'	C _s	4	91.12	−35.33	141.32
	1D'	C _{2v}	2	148.64	−49.71	198.83
VN ₉ ⁺	2A	C ₁	1	0	−30.83	138.74
	2B	C ₁	1	1.90	−31.25	140.64
	2C	C ₁	1	8.36	−32.69	147.10
	2D	C ₁	1	51.22	−42.21	189.96
VN ₉	2A'	C ₁	4	0	−21.39	96.28
	2B'	C ₁	2	10.92	−23.82	107.20
	2C'	C _s	4	59.24	−34.56	155.51
	2D'	C ₁	6	84.58	−40.19	180.85
VN ₁₀ ⁺	3A	C _s	3	0	−8.84	44.20
	3B	C _s	5	17.93	−12.43	62.13
	3C	C _s	1	181.28	−45.10	225.48
	3D	C ₁	3	208.83	−50.61	253.03
VN ₁₀	3A'	C ₁	2	0	−11.55	57.76
	3B'	C _s	6	29.89	−17.53	87.65
	3C'	C _{2v}	2	109.08	−33.37	166.84
	3D'	C ₁	2	123.19	−36.19	180.95

N=N double bond (1.25 Å). The \angle NNN angles in the N₄ ring are about 90°.

Some other all-nitrogen rings were also found in low-lying isomers of VN₈. Isomer 1B' is the next most stable structure of VN₈ with one end-on bound N₂, one linear N₃, and an η^3 -N₃ ring. It is 41.18 kcal/mol higher in energy than 1A'. The most stable isomer with a N₅ ring in VN₈ is 1C'. It contains an η^5 -N₅ ring and an η^2 -N₃ ring and exhibits C_s symmetry. The η^5 -N₅ ring in 1C' is aromatic with a N–N distance of 1.33 Å, which is similar to that in V(η^5 -N₅)₂ as reported by Tsipis et al. (1.346 Å).²⁷ The 1D' isomer has two N₄ rings coordinated to the V atom and displays a bent sandwichlike structure with eclipsed C_{2v} symmetry. It is worth mentioning that the structure of 1D' calculated in this work is in agreement with that obtained from previous theoretical calculations by Mercero et al.²⁵ Isomers 1C' and 1D' lie 91.12 and 148.64 kcal/mol higher in energy than isomer 1A', respectively.

3.2.2. Structures of VN₉⁺ and VN₉. As shown in Figure 3, the most stable isomer of VN₉⁺ (2A) consists of one nitrogen atom, two N₂ molecules, and one N₄ ring around the vanadium atom. The N₄ ring connects to the V atom through only two nitrogen atoms on one side (N1 and N2) and exhibits an isosceles trapezoidal structure with bond lengths of N1–N2, N3–N4, and N2–N3 (N1–N4) that are 1.33, 1.24, and 1.47 Å, respectively. The bond length of N3–N4 is very close to that of N=N (1.25 Å), whereas the bond length of N2–N3 (N1–N4) is close to that of N–N (1.45 Å). The N10 atom connects to the vanadium atom tightly with a short V–N10 distance of 1.48 Å. 2B is the second most stable structure with one N₂ molecule, one N₃ moiety, and one η^4 -N₄ ring. It lies 1.90 kcal/mol higher in energy than 2A. The η^4 -N₄ ring in 2B has a trapeziform structure with N–N bond lengths of about 1.37 Å. The next most stable isomer of VN₉⁺ is 2C, which has a composition similar to that of 2A. However, the N₄ ring in 2C interacts with the vanadium atom by all four nitrogen atoms. Moreover, it is

distinctly distorted from planar structure with a torsion angle of 13.4. The energy of isomer 2C lies 8.36 kcal/mol above that of isomer 2A.

We also found the N₃ ring in the obtained low-lying isomers of VN₉⁺, but we have not found any isomers containing the N₅ ring. The most stable isomer with multirings in VN₉⁺ is 2D, which is formed by adding one N₃ ring, one η^4 -N₄ ring, and one end-on bound N₂ molecule to the V atom. The N₃ ring connects to the V atom via only one nitrogen atom (N9) with a V–N₃ distance of 2.03 Å. The η^4 -N₄ ring in 2D has an irregular trapeziform structure with N–N bond lengths ranging from 1.35 to 1.39 Å. 2D exhibits C₁ symmetry and lies 51.22 kcal/mol in energy above isomer 2A.

For neutral VN₉, the low-lying isomers are similar to their positive counterparts. As shown in Figure 4, 2A' is the most stable structure with one N₂ molecule, one N₃ moiety, and one η^4 -N₄ ring. 2B' is the second most stable structure with one nitrogen atom, two N₂ molecules, and one η^4 -N₄ ring, lying 10.92 kcal/mol higher in energy than 2A'. In general, the structures of 2A' and 2B' are analogous to those of 2B and 2C, respectively. However, their η^4 -N₄ rings are coplanar, and the V–N₄ parts have leaning pyramidal structure. For 2A', the N–N bond lengths in η^4 -N₄ rings are concentrated in the small range of 1.36–1.38 Å. The V–N1(N2) and V–N3(N4) distances are 2.07 and 2.04 Å, respectively. As for isomer 2B', the vanadium atom is connected tightly to N1 and N2 with a short V–N1(N2) distance of 2.01 Å, whereas the V–N3(N4) connection is looser with a long distance of 2.27 Å.

Among the obtained low-lying states of VN₉, the N₃ and N₅ rings were also found and they tend to form multirings isomers. The most stable isomer with N₃ rings in VN₉ is 2C', which is very similar to 2D. The most stable isomer with the N₅ ring is 2D', in which a N₅ ring and another N₄ ring are coordinated to the V atom face to face. The sandwichlike structure of 2D' is reported for the first time as far as we know. η^5 -N₅ in 2D' is an

aromatic ring with a uniform N–N distance of 1.33 Å and a \angle NNN angle of 108.0°. η^4 -N₄ in 2D' also has a uniform N–N bond length of 1.36 Å, but it is distorted from planar structure with a torsion angle of 8.6°. The energy of isomers 2C' and 2D' lies 59.24 and 84.58 kcal/mol above that of isomer 2A', respectively.

3.2.3. Structures of VN₁₀⁺ and VN₁₀. The two most stable isomers of VN₁₀⁺ were shown to be 3A and 3B, in which 3B lies 17.93 kcal/mol above isomer 3A. They were all formed by adding three end-on bound N₂ units and one η^4 -N₄ ring to the V atom in different manners, and they all exhibit C_s symmetry. The structure of V–N₄ in 3A is slightly leaning pyramidal with V–N₄ distances of about 2.01–2.05 Å. The N₄ ring in 3A has isosceles trapezoid structure with N–N bond lengths of about 1.37 Å. In contrast, the N₄ ring in 3B is distorted from planar structure with a torsion angle of 13.2, and V–N₄ distances extend to 2.13–2.25 Å.

The most stable isomer with the N₃ unit in VN₁₀⁺ is 3C, which has two end-on bound N₃ units and one N₄ ring around the vanadium atom and exhibits C_s symmetry. The N–N bond lengths in N₃ moieties are 1.25 and 1.11 Å, which are similar to those in a typical azide. The N₄ ring and V–N₄ in 3C also have isosceles trapezoid and slightly leaning pyramidal structure, respectively. The energy of 3C is much higher than that of 3A by 181.28 kcal/mol. Among the low-lying isomers of VN₁₀⁺, we also found 3D with two η^4 -N₄ rings and one end-on bound N₂ molecule. It has C₁ symmetry and displays an eclipsed sandwichlike structure in which one N₄ ring is coplanar and the other one is obviously distorted with a torsion angle of 7.3. The energy of isomer 3D lies 208.83 kcal/mol above that of isomer 3A.

As shown in Figure 4, the constitution of neutral VN₁₀ isomers is analogous to that of their positive counterparts. The most stable isomer of VN₁₀ is 3A' with three end-on bound N₂ units and one η^4 -N₄ ring. The N–N bond lengths in the N₄ ring are almost the same (1.38–1.39 Å). The vanadium atom is located right above the coplanar N₄ ring with an equal V–N₄ distance of 2.03 Å. The second most stable isomer (3B') lies 29.89 kcal/mol above 3A', respectively. It exhibits C_s symmetry in which the position between the vanadium atom and N₄ ring is slipped and only two nitrogen atoms on one side of the N₄ ring interact directly with the vanadium atom. Consequently, the N–N bond in the N₄ ring connected to the vanadium atom has a length of 1.43 Å, which is very close to the N–N single bond (1.45 Å), whereas the neighboring bonds have lengths of about 1.29 Å, which are close to the N=N double bond (1.25 Å).

Among the obtained low-lying states of VN₁₀, the most stable isomer with a N₃ unit is 3C' with two end-on bound N₃ units and one η^4 -N₄ ring. The most stable isomer with multirings is 3D' with one end-on bound N₂ unit and two η^4 -N₄ rings. The structures of 3C' and 3D' are very similar to those of 3C and 3D, respectively. However, their η^4 -N₄ rings are nearly coplanar, and the N–N bond lengths in each N₄ ring are concentrated in a small range. Isomers 3C' and 3D' lie 109.08 and 123.19 kcal/mol in energy above isomer 3A', respectively.

4. DISCUSSION

4.1. Binding Energies of V–N Clusters. To estimate the strength of the interactions between the V atom and nitrogen ligands, we performed calculations on the binding energies of various VN_n⁺ and VN_n (*n* = 8, 9, and 10) complexes. The calculation results are listed in Table 1. For the low-lying

isomers of the VN₈⁺ cluster with four end-on bound N₂ units, the average binding energy (*E_b*) calculated with formula 1 refers to the bond energy between the vanadium cation and N₂ units. Therefore, on the basis of the calculated binding energy of the most stable structure of the VN₈⁺ cluster (24.84 kcal/mol, that is 1.08 eV), the energy of a 266 nm photon (4.66 eV) is able to dissociate four N₂'s from isomer 1A of the VN₈⁺ cluster. That is in good agreement with our photodissociation experiment, as the experiment showed that the photodissociation of VN₈⁺ at 266 nm can mainly remove eight nitrogen atoms (four N₂ molecules). The good agreement between the experiment and theoretical calculations validates the selection of the theoretical method in this work and confirms that the VN₈⁺ cluster detected in our experiment is in the form of V(N₂)₄⁺ with D_{4h} symmetry.

As seen from Table 1, the binding energies of the low-lying isomers of VN₈⁺ (1A, 1B) are positive, suggesting substantial energy stabilization of the VN₈⁺ species as compared to that of the bare vanadium cation and N₂ molecules. Furthermore, the binding energy of the ground state of VN₈⁺ (1A) is much higher than those of VN₉⁺ (2A) and VN₁₀⁺ (3A), indicating that the VN₈⁺ cluster would be more stable than the VN₉⁺ and VN₁₀⁺ clusters. These results are in good agreement with the mass spectrum obtained from the laser ablation experiment.

4.2. Structures of V–N Clusters. Several of the most stable structures of VN_n⁺ and VN_n (*n* = 8, 9, and 10) as well as some typical low-lying isomers with various all-nitrogen units have been shown in Figures 3 and 4. The end-on bound N₂ units are most common in them with a N–N bond length of about 1.09 Å, which is the same as that in nitrogen molecules calculated in this work. The N–N bonds in side-on bound N₂ units are obviously weakened by coordination with N–N bond lengths of about 1.13 Å. The N₄ rings are the second most common ligands in VN_n⁺ and VN_n (*n* = 8, 9, and 10) isomers. They can connect to vanadium only by one side (2A, 3B') or by a whole face with V located directly above them (1D, 3A'). In most cases, the relative positions of vanadium atoms and N₄ rings lie between the above two states, giving rise to leaning pyramidal V–N₄ structures. In addition, N₄ together with other all-nitrogen rings could interact with V to form sandwich-like structures, such as N₄VN₄ (1D') and N₄VN₅ (2D').

Regarding the N–N bond distances in N₄ rings of low-lying isomers, for nonpyramidal V- η^2 -N₄ structures (2A, 3B'), the presence of vanadium on the side of the ring induces alternating N–N distances, and these N₄ ligands can be regarded as a complex composed of two N₂ units. Specifically, the N₄ ring in 2A is formed by a side-on bound N₂ ligand with a N–N distance of 1.33 Å and an unbound N₂ unit with a N–N distance of 1.24 Å, while N₄ ring in 3B' is formed by two end-on bound N₂ ligands with a N–N distance of about 1.29 Å. The interaction between N₂ units in the above N₄ rings is relatively weak as the N–N distances are up to 1.43–1.47 Å, very close to the bond length of the N–N single bond (1.45 Å). For pyramidal V- η^4 -N₄ structures, all N–N bond distances are concentrated in a small range of 1.35–1.39 Å, especially around 1.37 Å, within the bond length of N–N single (1.25 Å) and double bonds (1.45 Å) and close to those in the bare N₄²⁻ ring (1.38 Å) calculated by Cheng et al.²⁴

4.3. Energy Properties of V–N Clusters. The N–N bond lengths of N₄ rings found in this work lie between those of the N–N single and double bonds. The \angle NNN angles in them are close to 90°. Therefore, as predicted by Cheng et al.,²⁴ the N₄ rings found in this work are energetic. To understand the high-

energy nature of the V–N clusters, we have calculated their formation energies with formula II. As shown in Table 1, the formation reactions of all isomers except 1A and 1B are endothermic, indicating that those clusters found in this work are all energetic species. More specifically, the ground state of VN_9^+ (2A) lies 138.74 kcal/mol higher in energy above a V cation and 9/2 N_2 molecules. Previously suggested ThN_6 ,³¹ ScN_7 ,³² and N_5ThN_7 ³³ lie approximately 72, 125, and 132 kcal/mol higher in energy than the corresponding atom and N_2 molecules, respectively. Therefore, isomer 2A observed in our experiment is energetically higher than the predicted metal nitrides. The most stable isomer of VN_{10}^+ (3A) gives an energy of 44.20 kcal/mol above a V cation and five N_2 molecules. As for the ground state of neutral clusters, VN_8 , VN_9 , and VN_{10} can release energies of about 50.20, 96.28, and 57.76 kcal/mol when they decompose into a V atom and a corresponding number of N_2 molecules, respectively.

Except for the N_4 rings, end-on bound N_2 molecules do not make any contributions to the energy of the above clusters, so converting the remaining N_2 ligands in V-doped nitrogen clusters could make them effective HEDMs. For example, the formation energies of isomer 1D' with a structure of $(\eta^4\text{-N}_4)\text{V}(\eta^4\text{-N}_4)$, isomer 2D' with a structure of $(\eta^4\text{-N}_4)\text{V}(\eta^5\text{-N}_5)$, and isomer 3C with a structure of $(\eta^4\text{-N}_4)\text{V}^+(\text{N}_3)_2$ are up to 198.83, 180.85, and 225.48 kcal/mol, respectively.

5. CONCLUSIONS

VN_8^+ , VN_9^+ , and VN_{10}^+ clusters were generated by a laser ablation experiment. The mass spectrometry showed that the abundance of VN_8^+ is much higher than those of VN_9^+ and VN_{10}^+ . The VN_8^+ cluster was further investigated by a photodissociation experiment with 266 nm photons. Density functional calculations were made to search for the stable structures of V–N clusters. The theoretical calculations found that the most stable structure of VN_8^+ is in the form of $\text{V}^+(\text{N}_2)_4$ with D_{4h} symmetry. The calculated binding energy is in good agreement with that obtained from the photodissociation experiments. The ground states of VN_8 , $\text{VN}_9^{+/0}$, and $\text{VN}_{10}^{+/0}$ all consist of a N_4 ring and exhibit an energetic nature. The most stable isomer of VN_9^+ is in the form of $(\eta^2\text{-N}_4)\text{V}^+(\text{N}_2)_2$ with C_1 symmetry, while that of VN_{10}^+ is $(\eta^4\text{-N}_4)\text{V}^+(\text{N}_2)_3$ with C_s symmetry. They lie 138.74 and 44.20 kcal/mol higher in total energy above a V cation and a corresponding number of N_2 molecules, respectively. For neutral VN_8 , VN_9 , and VN_{10} , $(\eta^4\text{-N}_4)\text{V}(\text{N}_2)_2$, $(\eta^4\text{-N}_4)\text{V}(\text{N}_3)(\text{N}_2)$, and $(\eta^4\text{-N}_4)\text{V}(\text{N}_2)_3$ are their ground states. The N_4 ring was found not only in the ground states of VN_9^+ and VN_{10}^+ , which have been detected in this work, but also in many low-lying isomers of VN_n^+ and VN_n ($n = 8, 9$, and 10). As a new all-nitrogen ligand, the N_4 ring would be an energetic building block for constructing nitrogen-rich compounds.

AUTHOR INFORMATION

Corresponding Authors

*E-mail: gzx204@sina.com (Zhongxue Ge).

*E-mail: wlzhu@mail.shcnc.ac.cn (Weiliang Zhu).

*E-mail: zhengwj@iccas.ac.cn (Weijun Zheng).

ORCID

Kewei Ding: 0000-0002-6301-2362

Weiliang Zhu: 0000-0001-6699-5299

Weijun Zheng: 0000-0002-9136-2693

Notes

The authors declare no competing financial interest.

ACKNOWLEDGMENTS

This work was supported by the National Natural Science Foundation of China (grant nos. 21103202, 21273246, and 21502148).

REFERENCES

- (1) Lauderdale, W. J.; Stanton, J. F.; Bartlett, R. J. Stability and energetics of metastable molecules: Tetraazetetrahedrane (N_4), hexaazabenzene (N_6), and octaazacubane (N_8). *J. Phys. Chem.* **1992**, *96*, 1173–1178.
- (2) Östmark, H. High energy density materials (HEDM): Overview, theory and synthetic efforts at FOI. *New Trends in Research of Energetic Materials Czech Republic* **2006**, 231–250.
- (3) Zarko, V. E. Searching for ways to create energetic materials based on polynitrogen compounds. *Combust., Explos. Shock Waves* **2010**, *46*, 121–131.
- (4) Samartzis, P. C.; Wodtke, A. M. All-nitrogen chemistry: How far are we from N_6 ? *Int. Rev. Phys. Chem.* **2006**, *25*, 527–552.
- (5) Glukhovtsev, M. N.; Jiao, H.; Schleyer, P. v. R. Besides N_2 , what is the most stable molecule composed only of nitrogen atoms? *Inorg. Chem.* **1996**, *35*, 7124–7133.
- (6) Christe, K. O.; Wilson, W. W.; Sheehy, J. A.; Boatz, J. A. N_5^+ : A novel homoleptic polynitrogen ion as a high energy density material. *Angew. Chem., Int. Ed.* **1999**, *38*, 2004–2009.
- (7) Cacace, F.; de Petris, G.; Troiani, A. Experimental detection of tetranitrogen. *Science* **2002**, *295*, 480–481.
- (8) Vij, A.; Pavlovich, J. G.; Wilson, W. W.; Vij, V.; Christe, K. O. Experimental detection of the pentaazacyclopentadienide (pentaazolate) anion, cyclo-N_5^- . *Angew. Chem., Int. Ed.* **2002**, *41*, 3051–3054.
- (9) Hansen, N.; Wodtke, A. M. Velocity map ion imaging of chlorine azide photolysis: Evidence for photolytic production of cyclic- N_3 . *J. Phys. Chem. A* **2003**, *107*, 10608–10614.
- (10) Hansen, N.; Wodtke, A. M.; Goncher, S. J.; Robinson, J. C.; Sveum, N. E.; Neumark, D. M. Photofragment translation spectroscopy of ClN_3 at 248 nm: Determination of the primary and secondary dissociation pathways. *J. Chem. Phys.* **2005**, *123*, 104305.
- (11) Wodtke, A. M.; Hansen, N.; Robinson, J. C.; Sveum, N. E.; Goncher, S. J.; Neumark, D. M. The Cl to NCl branching ratio in 248-nm photolysis of chlorine azide. *Chem. Phys. Lett.* **2004**, *391*, 334–337.
- (12) Samartzis, P. C.; Hansen, N.; Wodtke, A. M. Imaging ClN_3 photodissociation from 234 to 280 nm. *Phys. Chem. Chem. Phys.* **2006**, *8*, 2958–2963.
- (13) Zhang, P.; Morokuma, K.; Wodtke, A. M. High-level ab initio studies of unimolecular dissociation of the ground-state N_3 radical. *J. Chem. Phys.* **2005**, *122*, 014106.
- (14) Babikov, D.; Kendrick, B. K.; Zhang, P.; Morokuma, K. High-level ab initio studies of unimolecular dissociation of the ground-state N_3 radical. *J. Chem. Phys.* **2005**, *122*, 044315.
- (15) Prinzbach, H.; Fischer, G.; Rihs, G.; Sedelmeir, G.; Heilbronner, E.; Yang, Y.-Z. The azo-chromophore as component in photo [2 + 2]-cycloaddition reactions synthesis, structure and pe-analysis of planar-parallel bisazo-molecules. *Tetrahedron Lett.* **1982**, *23*, 1251–1254.
- (16) Exner, K.; Fischer, G.; Bahr, N.; Beckmann, E.; Luga, M.; Yang, F.; Rihs, G.; Keller, M.; Hunkler, D.; Knothe, L.; et al. Photochemical transformations, 83 proximate, syn-periplanar bisdiazene skeletons: Syntheses, structures, homoconjugate reactivity and photochemistry. *Eur. J. Org. Chem.* **2000**, *2000*, 763–785.
- (17) Cullmann, O.; Vogtle, M.; Stelzer, F.; Prinzbach, H. Proximate, syn-periplanar bisdiazenes/bisdiazeneoxides - syntheses, photochemistry. *Tetrahedron Lett.* **1998**, *39*, 2303–2306.
- (18) Fischer, G.; Fritz, H.; Rihs, G.; Hunkler, D.; Exner, K.; Knothe, L.; Prinzbach, H. Photochemical transformations, 82 proximate, syn-periplanar, rigid imine(nitrone)/ene-, and diazene(diazeneoxy)/ene systems: Syntheses, homoconjugate reactivity and photochemistry. *Eur. J. Org. Chem.* **2000**, *2000*, 743–762.

- (19) Exner, K.; Prinzbach, H. Highly efficient photometathesis in a proximate, synperiplanar diazene-diazene oxide substrate: Retention of optical purity, mechanistic implications. *Chem. Commun.* **1998**, 749–750.
- (20) Exner, K.; Fischer, G.; Lukan, M.; Fritz, H.; Hunkler, D.; Keller, M.; Knothe, L.; Prinzbach, H. Photochemical transformations, 84 proximate, syn-periplanar diazene/piazene(di)oxy, diazeneoxy/piazene(di)oxy, and diazenedioxy/piazenedioxy skeletons: Syntheses, [2 + 2] photocycloadditions, metathesis. *Eur. J. Org. Chem.* **2000**, 2000, 787–806.
- (21) Camp, D.; Campitelli, M.; Hanson, G. R.; Jenkins, I. D. Formation of an unusual four-membered nitrogen ring (tetrazetidine) radical cation. *J. Am. Chem. Soc.* **2012**, *134*, 16188–16196.
- (22) Van Zandwijk, G.; Janssen, R. A. J.; Buck, H. M. 6.pi. Aromaticity in four-membered rings. *J. Am. Chem. Soc.* **1990**, *112*, 4155–4164.
- (23) Li, Q. S.; Cheng, L. P. Aromaticity of square planar N_4^{2-} in the M_2N_4 ($M = Li, Na, K, Rb, \text{ or } Cs$) species. *J. Phys. Chem. A* **2003**, *107*, 2882–2889.
- (24) Cheng, L. P.; Li, Q. S. N_4 ring as a square planar ligand in novel MN_4 species. *J. Phys. Chem. A* **2005**, *109*, 3182–3186.
- (25) Mercero, J. M.; Matxain, J. M.; Ugalde, J. M. Mono- and multidecker sandwich-like complexes of the tetraazacyclobutadiene aromatic ring. *Angew. Chem., Int. Ed.* **2004**, *43*, 5485–5488.
- (26) Jin, L.; Ding, C.-h. $[N_3MN_3]^q$: A type of low-lying sandwich-like isomer on $[N_8M]^q$ hypersurface with (M, q) ($Ni, 0$), ($Co, -1$), and ($Fe, -2$). *J. Phys. Chem. A* **2009**, *113*, 13645–13650.
- (27) Tsiapis, A. C.; Chaviara, A. T. Structure, energetics, and bonding of first row transition metal pentazolato complexes: A DFT study. *Inorg. Chem.* **2004**, *43*, 1273–1286.
- (28) Lein, M.; Frunzke, J.; Timoshkin, A.; Frenking, G. Iron bispentazole $Fe(\eta^5-N_5)_2$, a theoretically predicted high-energy compound: Structure, bonding analysis, metal-ligand bond strength and a comparison with the isoelectronic ferrocene. *Chem. - Eur. J.* **2001**, *7*, 4155–4163.
- (29) Choi, C.; Yoo, H.-W.; Goh, E. M.; Cho, S. G.; Jung, Y. $Ti(N_5)_4$ as a potential nitrogen-rich stable high-energy density material. *J. Phys. Chem. A* **2016**, *120*, 4249–4255.
- (30) Straka, M.; Pyykko, P. One metal and forty nitrogens. Ab initio predictions for possible new high-energy pentazolides. *Inorg. Chem.* **2003**, *42*, 8241–8249.
- (31) Duan, H.-X.; Li, Q.-S. A series of novel aromatic compounds with a planar N_6 ring. *Chem. Phys. Lett.* **2006**, *432*, 331–335.
- (32) Gagliardi, L.; Pyykko, P. Scandium cycloheptanitride, ScN_7 : A predicted high-energy molecule containing an $[\eta^7-N_7]^{3-}$ ligand. *J. Am. Chem. Soc.* **2001**, *123*, 9700–9701.
- (33) Gagliardi, L.; Pyykko, P. $\eta^5-N_5^-$ -Metal- $\eta^7-N_7^{3-}$: A new class of compounds. *J. Phys. Chem. A* **2002**, *106*, 4690–4694.
- (34) Haiges, R.; Boatz, J. A.; Schneider, S.; Schroer, T.; Yousufuddin, M.; Christe, K. O. The binary group 4 azides $[Ti(N_3)_4]$, $[P(C_6H_5)_4]^-$, $[Ti(N_3)_5]$, and $[P(C_6H_5)_4]_2[Ti(N_3)_6]$ and on linear Ti-N-NN coordination. *Angew. Chem., Int. Ed.* **2004**, *43*, 3148–3152.
- (35) Haiges, R.; Boatz, J. A.; Schroer, T.; Yousufuddin, M.; Christe, K. O. Experimental evidence for linear metal-azido coordination: The binary group 5 azides $[Nb(N_3)_5]$, $[Ta(N_3)_5]$, $[Nb(N_3)_6]^-$, and $[Ta(N_3)_6]^-$, and 1:1 acetonitrile adducts $[Nb(N_3)_5(CH_3CN)]$ and $[Ta(N_3)_5(CH_3CN)]$. *Angew. Chem., Int. Ed.* **2006**, *45*, 4830–4835.
- (36) Haiges, R.; Boatz, J. A.; Yousufuddin, M.; Christe, K. O. Monocapped trigonal-prismatic transition-metal heptaazides: Syntheses, properties, and structures of $[Nb(N_3)_7]^{2-}$ and $[Ta(N_3)_7]^{2-}$. *Angew. Chem., Int. Ed.* **2007**, *46*, 2869–2874.
- (37) Haiges, R.; Boatz, J. A.; Christe, K. O. The syntheses and structure of the vanadium(IV) and vanadium(V) binary azides $V(N_3)_4$, $[V(N_3)_6]^{2-}$, and $[V(N_3)_6]^-$. *Angew. Chem., Int. Ed.* **2010**, *49*, 8008–8012.
- (38) Haiges, R.; Boatz, J. A.; Bau, R.; Schneider, S.; Schroer, T.; Yousufuddin, M.; Christe, K. O. Polyazide chemistry: The first binary group 6 azides, $Mo(N_3)_6$, $W(N_3)_6$, $[Mo(N_3)_7]^-$, and $[W(N_3)_7]^-$, and the $[NW(N_3)_4]^-$ and $[NMo(N_3)_4]^-$ ions. *Angew. Chem., Int. Ed.* **2005**, *44*, 1860–1865.
- (39) Filippou, A. C.; Portius, P.; Neumann, D. U.; Wehrstedt, K.-D. The hexaazidogermanate(IV) ion: Syntheses, structures, and reactions. *Angew. Chem., Int. Ed.* **2000**, *39*, 4333–4336.
- (40) Portius, P.; Filippou, A. C.; Schnakenburg, G.; Davis, M.; Wehrstedt, K.-D. Neutral Lewis base adducts of silicon tetraazide. *Angew. Chem., Int. Ed.* **2010**, *49*, 8013–8016.
- (41) Filippou, A. C.; Portius, P.; Schnakenburg, G. The hexaazidosilicate(IV) ion: Synthesis, properties, and molecular structure. *J. Am. Chem. Soc.* **2002**, *124*, 12396–12397.
- (42) Villinger, A.; Schulz, A. Binary bismuth(III) azides: $Bi(N_3)_3$, $[Bi(N_3)_4]^-$, and $[Bi(N_3)_6]^{3-}$. *Angew. Chem., Int. Ed.* **2010**, *49*, 8017–8020.
- (43) Knapp, C.; Passmore, J. On the way to “solid nitrogen” at normal temperature and pressure? Binary azides of heavier group 15 and 16 elements. *Angew. Chem., Int. Ed.* **2004**, *43*, 4834–4836.
- (44) Klapötke, T. M.; Krumm, B.; Scherr, M.; Haiges, R.; Christe, K. O. The binary selenium(IV) azides $Se(N_3)_4$, $[Se(N_3)_5]^-$, and $[Se(N_3)_6]^{2-}$. *Angew. Chem., Int. Ed.* **2007**, *46*, 8686–8690.
- (45) Klapötke, T. M.; Krumm, B.; Mayer, P.; Schwab, I. Binary tellurium(IV) azides: $Te(N_3)_4$ and $[Te(N_3)_5]^-$. *Angew. Chem., Int. Ed.* **2003**, *42*, 5843–5846.
- (46) Pillai, E. D.; Jaeger, T. D.; Duncan, M. A. IR spectroscopy of $Nb^+(N_2)_n$ complexes: Coordination, structures, and spin states. *J. Am. Chem. Soc.* **2007**, *129*, 2297–2307.
- (47) Pillai, E. D.; Jaeger, T. D.; Duncan, M. A. IR spectroscopy and density functional theory of small $V^+(N_2)_n$ complexes. *J. Phys. Chem. A* **2005**, *109*, 3521–3526.
- (48) Brathwaite, A. D.; Abbott-Lyon, H. L.; Duncan, M. A. Distinctive coordination of CO vs N_2 to rhodium cations: An infrared and computational study. *J. Phys. Chem. A* **2016**, *120*, 7659–7670.
- (49) Duarte, H. A.; Salahub, D. R.; Haslett, T.; Moskovits, M. $Fe(N_2)_n$ ($n = 1-5$): Structure, bonding and vibrations from density functional theory. *Inorg. Chem.* **1999**, *38*, 3895–3903.
- (50) Jin, J.; Wang, G.; Zhou, M.; Andradá, D. M.; Hermann, M.; Frenking, G. The $[B_3(NN)_3]^+$ and $[B_3(CO)_3]^+$ complexes featuring the smallest π -aromatic species B_3^+ . *Angew. Chem.* **2016**, *128*, 2118–2122.
- (51) Zhou, M.; Jin, X.; Gong, Y.; Li, J. Remarkable dinitrogen activation and cleavage by the Gd dimer: From dinitrogen complexes to ring and cage nitrides. *Angew. Chem.* **2007**, *119*, 2969–2972.
- (52) Ding, K. W.; Li, X. W.; Xu, H. G.; Li, T. Q.; Ge, Z. X.; Wang, Q.; Zheng, W. J. Experimental observation of TiN_{12}^+ cluster and theoretical investigation of its stable and metastable isomers. *Chem. Sci.* **2015**, *6*, 4723–4729.
- (53) Miyajima, K.; Yabushita, S.; Knickelbein, M. B.; Nakajima, A. Stern-gerlach experiments of one-dimensional metal-benzene sandwich clusters: $M_n(C_6H_6)_m$ ($M = Al, Sc, Ti, \text{ and } V$). *J. Am. Chem. Soc.* **2007**, *129*, 8473–8480.
- (54) Wang, J.; Acioli, P. H.; Jellinek, J. Structure and magnetism of V_nBz_{n+1} sandwich clusters. *J. Am. Chem. Soc.* **2005**, *127*, 2812–2813.
- (55) Kandalam, A. K.; Rao, B. K.; Jena, P. Geometry and electronic structure of $V_n(Bz)_m$ complexes. *J. Chem. Phys.* **2004**, *120*, 10414–10422.
- (56) Koyasu, K.; Atobe, J.; Furuse, S.; Nakajima, A. Anion photoelectron spectroscopy of transition metal- and lanthanide metal-silicon clusters: MSi_n^- ($n = 6-20$). *J. Chem. Phys.* **2008**, *129*, 214301.
- (57) Koyasu, K.; Atobe, J.; Akutsu, M.; Mitsui, M.; Nakajima, A. Electronic and geometric stabilities of clusters with transition metal encapsulated by silicon. *J. Phys. Chem. A* **2007**, *111*, 42–49.
- (58) Zhao, Y. C.; Zhang, Z. G.; Yuan, J. Y.; Xu, H. G.; Zheng, W. J. Modification of reflection time-of-flight mass spectrometer for photodissociation of mass-selected cluster ions. *Chin. J. Chem. Phys.* **2009**, *22*, 655–662.
- (59) Frisch, M. J.; Trucks, G. W.; Schlegel, H. B.; Scuseria, G. E.; Robb, M. A.; Cheeseman, J. R.; Scalmani, G.; Barone, V.; Mennucci,

B.; Petersson, G. A., et al. *Gaussian 09*, Revision A.02; Gaussian, Inc.: Wallingford, CT, 2009.

(60) Zhao, Y.; Truhlar, D. G. The M06 suite of density functionals for main group thermochemistry, thermochemical kinetics, non-covalent interactions, excited states, and transition elements: Two new functionals and systematic testing of four M06-class functionals and 12 other functional. *Theor. Chem. Acc.* **2008**, *120*, 215–241.

(61) Huenerbein, R.; Schirmer, B.; Moellmann, J.; Grimme, S. Effects of London dispersion on the isomerization reactions of large organic molecules: A density functional benchmark study. *Phys. Chem. Chem. Phys.* **2010**, *12*, 6940–6948.

(62) *CRC Handbook of Chemistry and Physics*; Haynes, W. M.; CRC Press: Boca Raton, FL, 2014–2015.